Planar cell polarity coordination in a cnidarian embryo provides clues to animal body axis evolution

Julie Uveira[1], Antoine Donati[2], Marvin Léria[1], Marion Lechable[1], François Lahaye[1], Christine Vesque[2], Evelyn Houliston[1] and Tsuyoshi Momose[1*]

1 Sorbonne Université, CNRS, Laboratoire de Biologie du Développement de Villefranche-sur-mer (LBDV- UMR7009), 181 Chemin du Lazaret, 06230, Villefranche-sur-Mer France
2 Sorbonne Université, CNRS UMR7622, INSERM U1156, Institut de Biologie Paris Seine (IBPS)-Developmental Biology Unit, 7-9 quai Saint Bernard, 75005, Paris, France
* Correponding authuor

Summary

Body axis specification is a crucial event in animal embryogenesis and was an essential evolutionary innovation for founding the animal kingdom. It involves two distinct components that coordinate to establish the spatial organisation of the embryo: initiation of cascades of regionalised gene expression and orientation of morphogenetic processes such as body elongation. Intense interest in the first component has revealed Wnt/β-catenin signalling as ancestrally responsible for initiating regional gene expression, but the evolutionary origin of oriented morphogenesis has received little attention. Here, by addressing the cell and morphological basis of body axis development in embryos of the cnidarian *Clytia hemisphaerica,* we have uncovered a simple and likely ancestral coordination mechanism between Wnt/β-catenin signalling and directed morphogenesis. We show that the ligand Wnt3, known to initiate oral gene expression via localised Wnt/β-catenin pathway activation, also has a key β-catenin-independent role in globally orienting planar cell polarity (PCP) to direct morphogenesis along the oral-aboral axis. This PCP orientation occurs in two distinct steps: local orientation by Wnt3 and global propagation by conserved core PCP protein interactions along the

body axis. From these findings we propose novel scenarios for PCP-driven symmetry-breaking underlying the emergence of the animal body plan.

Abbreviations

PCP: planar cell polarity. EG: early gastrula, LG: late gastrula, MO: Morpholino, OA: Oral-Aboral

Introduction

The earliest animals are thought to have been multicellular assemblages such as the "choanoblastaea", which evolved from a unicellular ancestor [1–4]. Subsequent evolutionary events that introduced a morphologically distinct primary body axis, i.e. breaking of tissue polarity symmetry, remain largely unaddressed (Fig.1A). In the animal lineage, Wnt/β-catenin-mediated specification of the primary body axis was likely an early innovation since it is found today across many species of both bilaterians (all of the animals' groups showing bilateral symmetry) and cnidarians (their sister group, comprising corals, sea anemones, jellyfish etc) [5–7]. Current evidence is insufficient to assess whether this innovation predated the branching of the more distantly related ctenophore and sponge clades [8,9]. Importantly, however, transcriptional activation by β-catenin and its partner TCF at one pole cannot alone explain the morphological component of axial tissue patterning. Rather, polarity information capable of directing axis development can be distributed globally across the whole embryo, as clearly illustrated by classic experimental manipulations in the hydrozoan *Clytia gregarium*, which led to the concept of global polarity [10]. Freeman's global polarity concept retrospectively has much in common with planar cell polarity (PCP), the mechanism coordinating the cell polarity in the plane of

epithelial tissues, later identified and unravelled genetically in *Drosophila* and vertebrates. PCP involves interactions between neighbouring cells, with each cell in a sheet, thus carrying polarity information. It is mediated by interactions of core PCP proteins: the Wnt receptor Frizzled (Fz), intracellular signal transducer Dishevelled (Dsh), transmembrane protein Strabismus/Van Gogh (Stbm), LIM-domain protein Prickle (Pk) and G-protein coupled receptor cadherin Flamingo (Fmi), to ensure tissue polarity and enable morphogenesis [11–15]. A conserved feature of PCP is the polarised localisation of the Stbm-Pk-Fmi complex on one side of the apical cortex of each cell and Fz-Dsh-Fmi complex on the other side. These two complexes interact between adjacent cells to coordinate PCP orientation of neighbouring cells. The PCP proteins are conserved across bilaterians and cnidarians, as well as in some sponge groups [16–18]. Fz and Dsh are both a core PCP component and the receptor for Wnt ligands in initiating Wnt/β-catenin signalling, so Wnt, Fz and Dsh are potentially key elements in coupling the pathways.

Two crucial issues both for the developing embryo, and for the earliest animal ancestors, are i) to orient PCP and thus morphogenesis consistently and globally across the whole embryo, and ii) to coordinate PCP orientation with regionalised cell fate specification initiated by Wnt/β-catenin signalling. These issues have not been addressed in the context of the primary body axis specification, while current examples of PCP orienting mechanisms from other tissues and animals show considerable variability [11].

We address here the coupling of Wnt signalling and PCP during body axis specification in a cnidarian in order to shed light on the roles of PCP in the evolutionary emergence of the metazoan body axis, exploiting the jellyfish model species *Clytia hemisphaerica* [19]. Previously, we showed that maternal mRNAs for

the ligand CheWnt3 (orthologue of bilaterian Wnt3, hereafter called Wnt3) and its receptors are localised with respect to the animal-vegetal polarity of the unfertilised *Clytia* egg (Fig. 1B), and activate Wnt/β-catenin signalling in a future oral (posterior) domain of the developing embryo to control gene expression along the developing primary body axis (oral-aboral: OA) [20,21]. In parallel, conserved core PCP proteins, including Stbm orthologue CheStbm (Stbm), are responsible for establishing tissue polarity (PCP) in the epidermis to support directed larval swimming via cilia beating along the oral-aboral axis, and are also required for elongation along the primary body axis during gastrulation [22]. Stbm protein is localised on the aboral side of each cell [22] as expected from *Drosophila* and vertebrate PCP deployment mechanisms. In the current work, we explore the hypothesis that Wnt3, as well as activating Wnt/β-catenin signalling [21], provides the initial cue to direct global orientation of PCP and thereby define the *Clytia* embryonic body axis both molecularly and morphologically. A first hint of this from our previous work was that the characteristic and complete absence of embryonic axis elongation observed following Wnt3 knockdown by Morpholino (Wnt3-MO) injection could be restored by injection of synthetic Wnt3 mRNA into single blastomeres during early development [21]. Importantly, Wnt3 is the sole Wnt mRNA detected before the early gastrula (EG) stage, the period when axial morphology and epidermal PCP are established, with other Wnt genes being expressed downstream of Wnt3 or at subsequent stages of larval development [21,23] (Fig.1B Fig. S1). This greatly facilitates the assessment of Wnt ligand function in directing PCP, in contrast to traditional model species where multiple Wnt ligands have parallel roles during embryogenesis. The studies reported here reveal how local Wnt3 cues orient the global axial PCP and PCP-driven oriented morphogenesis in the *Clytia* embryo. Two discrete steps define the PCP

orientation: a local cueing step with orally localised Wnt3 signal and a global propagation and coordination step mediated by core PCP proteins. Interestingly, while the role of Wnt3 is the instructive cue for PCP orientation and thus morphological axis development during *Clytia* normal development, other cues, including mechanical strains, can orient PCP. A similar variety of PCP orientation cues has been reported in *Drosophila* and vertebrates. Our findings allow us to propose a 'PCP-first' model for body axis symmetry-breaking in the metazoan ancestors, in which the self-organising activity of the PCP pathway allowed body axis innovation in early animal ancestors.

Results

A local Wnt3 cue orients global PCP

We first analysed in detail PCP in Wnt3-depleted embryos at the EG stage, the earliest stage that shows morphological OA polarity (Fig.1B, S1). PCP manifests as structural and positional asymmetries of the ciliary basal bodies, which are consistently positioned towards the oral side of the apical cortex. As previously [22], we quantified epidermal PCP orientation by assessing the basal body positioning (Fig.1D). In unmanipulated or control-MO-injected embryos, cells showed coordinated PCP, with 85% of cells orienting within ±45° (s.d. 33 and 34° respectively) of the average orientation. In embryos injected with Morpholino antisense oligonucleotides (Wnt3-MO) to block Wnt3 translation, PCP was oriented nearly completely randomly (Fig.1E, F) (s.d. 84°, comparable to 95° for Stbm-MO embryos [22]), and individual cells were less polarised (Fig.1G), reflecting the complete lack of axial morphology. The apical cell boundary was wrinkled in Wnt3-MO-injected cells (Fig. 1E), as observed following Fz1-MO, Dsh-MO or Stbm-MO-injections [22], indicative of markedly reduced cortical tension. These analyses demonstrate that

Wnt3 depletion causes PCP defects equivalent to the knockdown of the core PCP proteins [22]. This supports the hypothesis that Wnt3 provides a local cue to orient global PCP, which is responsible for the development of cilia polarity and axially elongated morphogenesis in *Clytia*.

To test this hypothesis, we injected Wnt3 mRNA and fluorescently labelled Dextran into one blastomere at the four-cell stage in Wnt3-MO embryos, which we call the "Wnt3-rescue" experiment (Fig.1H, J). At the EG stage, we quantified PCP in a broad area (246 x 246 μm) and represented it by bars with a circular colour code (Fig.1I). Control mock injections did not affect the PCP defects caused by Wnt3-MO. In contrast, coordinated PCP was restored by Wnt3 rescue in a non-autonomous manner (Fig. 1J). Restored ciliary alignment was observed at least 200 μm away from the Wnt3 mRNA-positive area. The Wnt3 source likely influences PCP at even further distances as a virtually complete morphological axis was restored by the late gastrula stage, with the Wnt3-mRNA lineage forming a new oral pole (Fig.1K) as shown previously [21]. Locally expressed Wnt3 signal is thus necessary and sufficient to orient the PCP along the whole body axis.

Rapid global PCP development precedes basal body alignment

To understand the initial process by which PCP becomes coordinated by Wnt3, we examined stages preceding EG, again using basal body localisation as the read-out. We reasoned that if PCP propagation occurs through successive cell interactions, cell alignment might spread as a wave across the embryo. PCP was detectable from the mid-blastula stage (8-9 hpf Fig. 2A-D), slightly after the onset of the zygotic Wnt3 expression [21] and epithelialisation of the blastula cells [24]. We did not, however, detect any wavefront of local cell alignment; rather, the PCP gradually increased in

coherence across the embryo over time (Fig.2A, B). This was confirmed by live imaging, injecting synthetic mRNAs in the egg to visualise cell contours with PH-Venus and basal bodies with Poc1-mCherry (Fig. 2E, Movie S1). The movies further revealed active mitosis in the blastodermal cells. A weak bias in cleavage orientation was observed along the OA axis (Fig. 2F). During mitosis, duplicated centrioles from the ciliary basal bodies are deployed in the mitotic spindles (Fig. 2E, Movie S1) such that basal body positioning becomes scrambled immediately after mitosis. Subsequently, the displaced basal bodies migrate unidirectionally toward the oral side of each cell, where the cilium is re-established, a clear indication that PCP was already in place across the tissue (Fig 2E, G, H). Together these observations indicate that PCP is established at the mid-blastula stage, presumably via canonical localisation of core PCP proteins to opposite cortices of each cell through continuous Fz-Stbm interaction. The protein partitioning then manifests as asymmetric basal body positioning. Localised PCP proteins may attract basal bodies to the oral cortex of the cell as described in ascidian embryos [25]. During subsequent stages, PCP is either maintained [26] in each cell during mitosis or rapidly restored through interactions with neighbouring cells [27].

Wnt3 orients PCP in a β-catenin-independent manner.

We previously showed that local Wnt3 expression is necessary and sufficient to activate the Wnt/β-catenin pathway in the oral pole of the *Clytia* embryo [21]. We next examined whether the action of Wnt3 for PCP orientation and morphogenesis is mediated by the Wnt/β-catenin pathway. First, we showed that PCP orientation by Wnt3 is independent of β-catenin: ectopic Wnt3 could orient PCP in the Wnt3-rescue experiment even in the presence of a dominant-negative form of CheTCF (dnTCF)

(Fig.3A), which blocks downstream transcription of the β-catenin pathway. Gastrulation was completely prevented, confirming that the Wnt/β-catenin pathway was inactive (Fig. 3C, D, Fig. S2). Furthermore, body axis elongation was partially restored at the early gastrula stage in the absence of an active β-catenin pathway (Fig. 3C), although they did not develop pointed morphology of the oral pole nor elongate further (Fig. 3D, Fig.S2). These results support a model in which axial elongation requires both PCP coordination and gastrulation (migration and intercalation of ingressed endodermal cells), as suggested previously [24]. Conversely, we found that constitutively active β-catenin (CA-β-cat) mRNA was not able to restore PCP coordination nor elongation of Wnt3-depleted embryos (Fig.3B) but did restore β-catenin-dependent gastrulation (Fig. S2). Taken together, these experiments demonstrate that global PCP orientation along the *Clytia* OA axis by Wnt3 is not mediated by the Wnt/β-catenin pathway. Wnt3 thus has dual independent roles: PCP orientation and Wnt/β-catenin activation.

Global PCP is established in two distinct steps.

We next tested the contribution of the core PCP proteins CheStbm and CheFmi (hereby called Stbm and Fmi) to linking PCP orientation to the local Wnt3 source. As expected, locally confined expression of Wnt3 mRNA did not restore global PCP coordination in Stbm-MO or Fmi-MO embryos (Fig.3E, F). Importantly, however, polarity was restored in the area immediately adjacent to the Wnt3 mRNA-positive cell patch. The effect covered a distance of a few cells, potentially derived from cells directly in touch with the Wnt source at earlier stages. This observation raised the possibility that global PCP orientation in *Clytia* embryos is established in two steps: Stbm/Fmi-independent PCP orientation by local Wnt3 at the oral end, followed by

global PCP propagation through the intercellular interaction of core PCP proteins (two-step model), as predicted by the domineering non-autonomy property of mosaic PCP mutations [28]. Alternatively, Wnt3 may diffuse from the oral Wnt3-expressing cells (Fig.1A) to form a long-range gradient along the OA-axis and orient the PCP (Wnt-gradient model). Wnt activity gradients have been shown to control or orient PCP in mice [29,30].

To distinguish these two models, we created mosaic embryos with a small patch of core-PCP negative cells within Wnt3-rescued embryos.

To achieve this, we transplanted single 32- or 64-cell stage blastomeres from Stbm-MO/Wnt3-MO or Fmi-MO/Wnt3-MO injected embryos to Wnt3-rescued embryos with Dextran lineage markers (Fig. 4A-E). The two-step model predicts that the PCP orientation would make a detour around the Stbm-MO/Fmi-MO mosaic area; in contrast, under the Wnt-gradient model, PCP would be affected only in the mosaic area. We found that in the Stbm-MO or Fmi-MO mosaic Wnt3-rescued embryos, PCP was correctly oriented or slightly disturbed within the Stbm-MO patch while often de-polarised in the Fmi-MO patch. Outside the Sbtm-MO or Fmi-MO patches, PCP orientation was inverted on the aboral side of the patches unless these were in close proximity to the Wnt3-mRNA patches. Stbm- or Fmi-defected cells thus exhibited domineering non-autonomy effects. This is consistent with the intercellular Fz-Fmi and Sbm-Fmi interaction model shown in *Drosophila* and vertebrates and the localisation of Stbm protein on the aboral side of each epidermal cell in *Clytia* [22]. PCP was oriented normally in the cells on the oral or lateral sides of the patches (Fig. 4B, D). PCP orientation from oral to aboral detouring around the Stbm-negative patches was similarly observed when mosaics were generated by injection of Stbm-MO into a single blastomere in a Wnt3-rescue embryo at the 16-cell stage (Fig.4F,

G). These observations strongly support the two-step model in which Wnt3 acts locally to orient PCP, and PCP coordination is then transmitted from oral (i.e. Wnt3-positive lineage) to aboral through core PCP interactions. They are not compatible with the alternative model that a long-range Wnt3-gradient orients PCP.

Mechanical cues can orient PCP.

Transplantation of Wnt3-MO blastomeres into Wnt3-MO host embryos at the 32- or 64-cell stage did not cause any PCP defects in most cases. However, in a few cases (N=3 out of 8), reorientation of PCP toward the transplanted donor lineage was observed (Fig.5A-E). In these cases, the donor cells were incompletely incorporated into the host ectodermal epithelium (Fig. 5D), such that the donor cells remained as a protrusion with a "rosette" (radial) arrangement. In these embryos, host and donor-derived epithelial cells acquired an elongated morphology around the circumference of the smooth host-donor boundary (Fig.5B). Although the grafted tissue influenced the orientation of PCP in the surrounding host cells, the direction was opposite to that driven by Wnt3-expressing sources. The rosette-like transplants thus operate as artificial “aboral” cues, in contrast with Wnt3 sources, which provide an oral cue (Fig. 5C). Unlike Stbm-MO or Fmi-MO mosaic embryos, cell polarity was continuous across the host-transplant border in these Wnt3-MO to Wnt3-MO transplantations (Fig.5A), suggesting the core PCP protein interaction was not disturbed at the boundary and thus not likely due to the nonautonomous effect of PCP defects. Epithelial ‘scarring’ can thus act to orient PCP, perhaps via discontinuities in cell adhesion or mechanical strain. PCP re-orientation by mechanical strain has been reported in wing PCP repatterning in *Drosophila* and for the orientation of *Xenopus* epidermal motile cilia [31–35]. We also performed transplantations into Wnt3-MO-only

hosts but did not obtain any such rosettes, so we could not determine whether Wnt has a permissive role for PCP in this context. Nevertheless, we can conclude that any local PCP asymmetry can potentially act as a PCP orientation cue via core-PCP proteins, and thus again is consistent with the two-step orientation model.

To explore further whether mechanical strain can orient PCP, we disrupted the morphology of the embryo by expressing dominant negative and constitutively active forms of *Clytia* RhoABC, the single cnidarian orthologue of the vertebrate Rho GTPases including RhoA. Late gastrula embryos expressing dominant negative RhoABC showed defects in axial elongation, consistent with a role in morphogenesis. Conversely, embryos injected with constitutively active RhoABC showed a scrambled axial morphology with ectopic protrusions induced along the major axis (Fig.5F). The induced protrusions appeared prior to gastrulation. PCP orientation was locally coordinated along the micro-axes of each protrusion so that they became extra aboral poles with respect to PCP (Fig.5G, H), while PCP orientation along the major body axis was globally maintained. Enhanced cortical actin fibres were arranged around the circumference of the induced protrusion (Fig. 5I). This method to provoke mechanical deformation of the embryo thus generated protrusions that mimicked the morphological extension and circumferential cell arrangement seen in the transplantation-induced rosettes, with in both cases PCP orientation aligning along the experimentally formed ectopic mini-axes.

Discussion

In this study, we have shown that during embryogenesis in the cnidarian *Clytia,* the ligand Wnt3, known to initiate oral gene expression via Wnt/β-catenin pathway

activation, also provides β-catenin-independent cues to orient PCP globally in the embryo and thereby direct morphogenesis along the oral-aboral axis. PCP orientation occurs in two distinct steps: local orientation by Wnt3 and global propagation via conserved core PCP machinery. These findings demonstrate deep conservation of PCP orientation and tissue morphogenesis mechanisms in eumetazoans, and allow us to novel scenarios for PCP-driven axis symmetry-breaking underlying the emergence of the animal body plan.

A single Wnt ligand coordinates molecular and morphological axis determination

Wnt/β-catenin signalling [5–7] and PCP pathway components [14,22,36–38] are involved respectively in embryonic body axis specification and morphogenesis across many metazoan species, but how these aspects are linked has been complicated to address. For instance, in vertebrates, Wnt5a and Wnt11 play crucial roles during body axis morphogenesis, [39–42] but it is not straightforward to demonstrate whether they provide positional cues to orient PCP along the body axis, while they do in other contexts (eg. orientation of ciliated node cells and muscle fibre) [30,43]. During *Clytia* embryogenesis, a single Wnt ligand directs both molecular and morphological aspects of axis formation. Wnt3 translated from maternally localised mRNA controls axial gene expression along the body axis via β-catenin regulation [21]. This dual role of the Wnt3 elegantly ensures the coherence of gene expression along the developing OA axis with morphogenetic aspects such as embryo elongation during gastrulation and beating of ectodermal cilia for directed locomotion. Maternal XWnt11 in *Xenopus* activates the Wnt/β-catenin pathway [44], and it is also implicated in the β-catenin-independent role to control convergent extension [39]. The dual roles

of a Wnt ligand for PCP and Wnt/tβ-catenin pathway may be a common strategy in vertebrates and cnidarians.

Two-step PCP orientation, initiated by CheWnt3 and propagated by core PCP interactions.

The experiments presented here reveal two distinct steps of Wnt3-driven PCP and axial morphology in *Clytia* embryos (Fig.6A): A Wnt3-dependent local PCP orientation (cueing) step is followed by a propagation step mediated by core PCP proteins. This resembles the “domineering non-autonomy” phenomenon described in *Drosophila* mosaic mutants for core PCP genes [28]. How Wnt3 locally orients PCP in the cueing step in *Clytia* embryos remains to be understood. A likely candidate is CheFz1 (a single orthologue to vertebrate Fzd1/2/7/3/6), whose predicted localisation is on the oral side of each cell, opposite to the aboral accumulation of Stbm. An attractive hypothesis is that Wnt3 from the oral pole anchors CheFz1 at the oral side of the cells adjacent to the Wnt3 source in a mechanism similar to zebrafish Wnt11 that locally accumulates Fz7 in the plasma membrane [45]. A further implication of the two-step model and the domineering non-autonomy character of PCP proteins is that PCP orientation may act as a morphogen-independent body axis maintenance mechanism in certain regeneration contexts in cnidarians [10,46,47]. Established local PCP coordination may be propagated to restore the body axis in regeneration. In this context, it would be interesting to investigate the mechanism by which core PCP modulates axial gene expression. In *Clytia*, PCP defects resulting from Stbm knockdown led to changes in gene expression at the early gastrula stage, notably affecting cells in the oral pole that ingress during gastrulation [23].

Conservation of the PCP orientation and morphogenesis mechanisms in metazoans.

In the *Drosophila* wing disc, local membrane-tethered Wg/Wnt4 in the wing margin can globally orient the PCP [48,49]. In vertebrate tissues, Wnt ligands either act as global cues for PCP orientation [30,43,50], or triggers involved in the body elongation [39–42]. The role of Wnt for PCP orientation is thus common across cnidarians and bilaterians. The Wnt subtypes employed in PCP orientation are, however, not conserved. The Wnt gene family gained its complexity prior to the bilaterian-cnidarian bifurcation [51]. Then, different Wnt subtypes were likely co-opted in different taxa and developmental contexts.

Other cues than Wnt also function as PCP orientation cues in the animal kingdom. In the developing *Drosophila* eye and abdomen, another signalling module comprising the atypical cadherins Fat(Ft) and Dachsous(Ds) and kinase Four-jointed(Fj) regulate the localisation of core PCP complexes via gradients of Ds and Fj [52,53]. Cnidarians have conserved Ft and Ds ortholog genes. In hydra Fat-like protein (HyFat1) is implicated in epithelial cell alignment and adhesion [54]. In *Clytia,* inhibition of Fat-like (CheFat1) and Ds (CheDs) disrupted global PCP coordination, and the Ds disruption was restored by Wnt3 expression (Fig.S3), suggesting that these molecules participate in global PCP orientation in a manner yet to be studied.

Besides molecular signalling cues, mechanical constraints or fluid flow are also known to direct PCP [31–35] and can potentially act as the PCP symmetry-breaking factor. The availability of alternative PCP orientation cues might have allowed evolutionary flexibility to link PCP to available structures, such as the cell polarity scaffold of eggs. While tissue polarity orientation by PCP is strongly conserved, the cellular mechanisms underlying the morphogenetic movement are highly variable.

Oriented cell division or convergent extension are likely major driving forces of blastula elongation prior to gastrulation in *Podocoryne carnea* {Momose.2005}, another hydrozoan jellyfish. In contrast, in *Clytia*, elongation likely involves PCP-dependent intercalation of both ectoderm [55] and ingressing endoderm [56] cells during gastrulation. In *Nematostella*, hydraulic pressure created by body wall muscle, organised along the body axis, drives the elongation [57] (Fig. S4)

Body axis symmetry-breaking in the evolutionary history of metazoa

The dual role of Wnt3 and the two-step PCP orientation mechanism revealed here are particularly intriguing in the context of understanding the emergence of animal body axes during evolution. The metazoan ancestor is considered to have taken a multicellular state such as a “choanoblastaea” from a unicellular ancestor [2,58] (Fig. 6B). Then metazoans acquired a body axis and germ layers and formed a hypothetical ancestral state such as Haeckel’s "gastraera" [59] or Hyman’s "planuloid-acoeloid" [60]. Early multicellular ancestors thus acquired morphological axis patterning and coupled it with regional gene expression. It is tempting to speculate that the β-catenin/TCF-dependent local gene expression and morphogenetic patterning coordinated by core PCP proteins were independently acquired and coupled by co-opting Wnt ligands and signal transducers from one pathway to the other. For example, Wnt, Fz and Dsh might have first been employed in the Wnt/β-catenin pathway, then recruited to a primordial PCP regulatory system (Fig. 6B). Genome analyses indicate that PCP effectors and a part of core PCP components such as Cdc42, RhoA, ROCK, Prickle or Inversin are evolutionarily older than metazoans [17] (Fig. S5, Table S1). Wnt-Fz-Dsh would then have been recruited to create morphogenesis machinery directed by PCP based on the existing local gene

expression by Wnt/β-catenin signalling. Alternatively, core PCP interactions and Wnt-driven PCP orientation may be more ancestral with Wnt-Fz-Dsh used in PCP orientation prior to its involvement in “canonical” Wnt signalling, acquired later though recruitment of the cell adhesion molecule β-catenin and its interaction with the DNA-binding TCF. Comparisons of the genomic repertoires for these components between species from across the metazoan phylogeny do not allow us to conclude which modules were acquired first (Fig.S5, S6, Table S1). In the outgroups of the cnidaria-bilateria clade, a full set of core PCP proteins are present in a sponge *Oscarella carmera* [17,18,61], and full Wnt/β-catenin pathways were identified in both Porifera and Ctenophora, while multiple cases of loss of Stbm/Fmi occurred in Porifera and potentially in Ctenophora (Fig.S5, Table S1).

PCP is a fundamental character in multicellular tissue organisation seen wide across metazoans (Fig. S5, S6) and may have been particularly important in the metazoan ancestor with lower anatomical complexity. It is known that a rotational polarity of the flagellar basal body is coordinated across the spheroid of green alga *Volvox carteri*, which thus independently acquired PCP-like character [62] (Fig.S6), suggesting that a PCP equivalent evolved independently in *Volvox*. PCP-driven axis evolution is an attractive scenario and can explain how an initial “choanoblastaea” multicellular ancestor acquired coordinated cilia/flagella flow. For example, PCP regulation might initially have improved filter-feeding efficiency in a choanoblastaea ancestor [2,63]. A comparative cell biology, or “Cellular Evo-Devo” approach, of the PCP/tissue polarities in diverse metazoans, in particular "basal metazoans" including Cnidaria, Ctenophora and Porifera, will be the key to addressing how symmetry-breaking to create a body axis arose during evolution.

Acknowledgements

This work was supported by ANR DiploDevo (ANR-09-BLAN-0236-01) and by the CNRS INSB Diversity of Biological Mechanisms program. We thank the IMEV Aquarium Service platform for maintaining and providing *Clytia* resources and the PIM platform for imaging. We thank Brandon Weissbourd for the critical reading of the manuscript.

Author Contributions

TM designed the project. TM and EH wrote the manuscript. TM, AD, JU and MLé performed the experiments. MLe, FL prepared *Clytia* animal setup. FL prepared plasmid vectors. TM, JU and MLé performed image data analysis. TM, EH and CV acquired funding.

Declaration of Interests

The authors declare no competing interests.

Materials and methods

Animal culture and embryo preparation.

Animal culture methods are described in [64]. Laboratory strains Z4B (female), Z4C2 (male) and their offspring (Z23/Z30) were used, provided by the EMBRC-Fr Aquarium Service. Daily spawning was induced by light with a 24-hour day-night cycle. Eggs and sperm were separately collected from jellyfish and transferred into 10 cm glass dishes two hours after the light stimulation. Eggs were fertilised less than one hour after the spawning. To acquire EG stages, embryos were incubated at 16°C for 18 hours, which corresponds to the 12~13 hpf stage at the standard culture temperature (18°C).

Microinjection

Morpholinos and mRNA were microinjected into unfertilised eggs or blastomeres at 4-cell ~ 16-cell stages using an Eppendorf Femtojet microinjector with

microcapillaries pulled with Narishige PN-30 needle puller. The tip of the needle was broken by touching it to a glass surface scratched by a diamond pen to open the needle tip to give an outer diameter of 2 to 4 μm. Eggs were aligned in a microinjection chamber made by casting and polymerising PDMS in a negative mould printed with a Form3 3D printer. 2~3% of the egg/cell volume of solution was injected by inserting a microcapillary needle with constant back pressure (Femtojet compensation pressure). It typically takes 0.5~1 seconds for each egg at 5~10 kPa when the needle has an appropriate opening size. The volume of injection for each injection was visually controlled under an Olympus SZX6 stereomicroscope with SZ-ILLT oblique illumination. 3~5 mg/ml lysine fixable 10 kDa Dextran labelled with Alexa647 or Cascade Blue were co-injected with Wnt3 mRNA and Stbm-MO/Fmi-MO for the lineage tracking in the Wnt3-Rescue experiment and PCP mosaic experiments.

Plasmid construction

Mutant and fluorescent protein templates were constructed in pCX3 vector, which contains short 5' and 3'UTR sequences from CheStbm mRNA. Wildtype CheWnt3 with 3 mispaired nucleotide residues at the Morpholino target and CheTCF lacking amino acid residues 2-27 (dnTCF) as a dominant negative form (lacking β-catenin binding site) of human TCF-4 [65] were amplified by PCR and cloned into the vector. A constitutively active form of Che-β-catenin (CA-β-cat) was created by introducing S97A T101A S105A mutations corresponding to the constitutively active mice β-catenin mutant lacking a GSK3-β phosphorylation target [66]. Constitutively active forms (CA1: G14V, CA2: Q63L) that gave identical phenotypes and a dominant form (DN: T19N) of CheRhoABC were designed based on the identical vertebrate RhoA mutants with the known phenotypes. These point mutations were introduced into wildtype cDNA clones in pCX3 vector using the QuickChange site-directed

mutagenesis kit (Stratagene). Poc1-mCherry and PH-domain-Venus fusions were constructed in a transgenic pMiniTol2-ACT2 vector [67] using NEBuilder Assembly kit from individually amplified PCR products or synthetic genes. mRNA was synthesised in vitro using mMessage mMachine T3 kit and poly(A)-tailing kit (Thermo Fisher) from PCR products amplified from the plasmids.

Immunostaining

Immunofluorescent visualisation of PCP by gamma-tubulin antibody and phalloidin staining was described previously [22]. List of the antibodies are in the Supplementary method. In brief, the embryos were fixed with 4% Paraformaldehyde in 0.1 M Hepes, 50 mM EGTA, 80 mM Maltose, 10 mM $MgSO_4$, 0.1% Triton X-100 and washed in PBST (1x PBS with 0.1%Triton X-100) then incubated in antibody solution in 1% BSA fraction V in PBST, followed by three times of washes for at least 5 minutes in PBST. After removing the detergent by washing in PBS, actin was stained with fluorescently labelled phalloidin in PBS (0.13 μM). After staining, embryos were cleared and mounted in Citiflour AF-1 diluted with an equal volume of PBS and scanned using Leica SP5 or Stellaris confocal microscopes with 63x objectives. The surface of the ciliated epidermis was Z-scanned (up to 10 μm) in the entire 246 x 246 μm field of view and z-stacked to visualise cell contour with apical cortical actin and basal body, typically at 0.081 μm resolution in XY-axis and 0.5~1 μm resolution in Z-axis.

Image analysis

The x-y coordinates of the apical surface centroid (x_c, y_c) of each cell and basal body of its cilium (x_b, y_b) are identified from the z-stacked confocal images. Detailed procedures and ImageJ scripts are described in the supplementary method. The polarity angle θ for each cell was calculated as

$$\theta = atan2(y_c - y_b, x_c - x_b)$$

The mean orientation (arrow in the radar plot) and circular standard deviation (circ. s.d.) are calculated [68]. A Matlab script was used to summarise the PCP orientation and statistics (Supplementary Method). The morphology of embryos in three dimensions (Figure. 5D, H) is reconstructed from a series of cortical actin confocal images by building a surface of the volume containing the cortical actin signals using Imaris software (Oxford Instruments).

Figure legends

Figure 1 Local Wnt3 globally orients the body axis tissue polarity and morphogenesis

(A) A key unanswered question of animal evolution is the origin of body axis patterning mechanisms, allowing initial multicellular assemblages to position specialised cell types (red) and coordinate cell polarity (represented in this diagram by oriented cilla and elongated shape) (B) Key stages of the early morphogenesis of *Clytia* embryos in relation to Wnt3 mRNA localisation (red). At the early gastrula (EG) stage, ectodermal cilia have formed, PCP has developed along the future oral-aboral axis, and the pointed morphology of the animal pole morphology can first be distinguished. Most axial elongation takes place during gastrulation. See also Supplementary Figure 1. (C) Schematic representation of planar cell polarity in a single epidermal cell at the EG stage. Basal bodies are positioned on the oral side at the apical cortex (translational polarity). (D) Confocal image of the apical surface of a single epidermal cell stained for actin (cyan, phalloidin labelling) and γ-tubulin immunostaining (magenta), and a representation of the PCP vector, defined by the basal body position and its mirror image across the apical surface centroid as the initial and terminal points, respectively. (E) Local PCP coordination in Control-MO

and Wnt3-MO-injected embryos at the EG stage. bar= 10 μm. Top) Confocal images as in D. Bottom) PCP vector representation of the cells in the images. Dots represent cells with no clear polarisation or mitotic cells. Apical cell contours are wavy in Wnt3-MO embryos. (F) Distribution of cell orientation in individual scans (lines) and their average (histogram) for non-injected (373 cells, 7 images), control-MO injected (304 cells from 3 images) and Wnt3-MO-injected (225 cells from 6 images). The average orientation is defined as the origin (0°) for each scan. Horizontal bar: standard deviation. G) The PCP polarisation index (degree of the polarisation of cells) by the length of the PCP vector, normalised by the cell size. See supplementary method for the definition (**** $p < 0.0001$, Mann–Whitney U test). (H) Experimental procedures of the Wnt3-rescue experiment. Wnt3MO is injected into unfertilised eggs, then rescue mRNA solution with fluorescently labelled 10 kDa dextran is injected into a 4-cell stage blastomere. (I) Circular colour-code representation of the PCP. (J) Wide range PCP coordination observed in Wnt3-rescue experiments. Left: Mock rescue control by water injection (N=9). Right: Rescue by Wnt3 mRNA injection (N=27). Each set consists of three illustrations. top: colour-wheel representation of the PCP. Cells derived from the Wnt3 or water-injected blastomere are at the top-right of each image, indicated with grey shading. bar= 50 μm. bottom-left: confocal thumbnail image. cyan: actin; yellow: Dextran-Alexa647(injected blastomere derived cells). bottom-right: radar plot of the cell orientation. The arrows in the radar show the circular mean of the PCP orientation within the single scan. circ s.d.: circular standard deviation. (K) Axial morphology of normal, Wnt3-MO injected and Wnt3 rescued embryos at late gastrula (LG) stage. bar=50 μm. Elongated body axis morphology was restored so that cells with injected Wnt3 mRNA were located at the induced oral (posterior). See also Fig. 3C.

Figure 2 Wnt3-driven PCP orientation precedes visible cell alignment.

(A, B) PCP orientation in Wnt3 rescue embryo at the mid-blastula stage (A: 8 hpf, N=10) and late-blastula stage (B: 9 hpf, B, N=10). Graphical PCP representations and radar histogram plots are as in Fig. 1. (C, D) Radar plot of PCP in distal (C) and proximal (D) areas of the region shown in (B). (E) Basal body displacements after cell divisions. Bar=10 μm. Cell membranes labelled by PH-Venus (green) and basal bodies with Poc1-mCherry (magenta). Arrows indicate basal bodies positioned on opposite sides of cleavage planes located after being engaged to the spindles. Aborally displaced basal bodies migrate toward the oral side. The average PCP defined the oral-aboral axis. (F) Distribution of the angles between the cleavage orientation axis to the OA axis defined by the PCP orientation (0-90°, n=131). Cleavages along the OA axis (0-45°) are favoured (* $p<0.05$ chi-square test). (G) Directional migration of the basal body toward the oral cell boundary after the cell cleavage. Each line indicates the distance of a single basal body to the oral edge of the cell after the last cleavage. Basal bodies migrate toward the oral cell boundary, suggesting PCP has been established by the time PCP becomes structurally manifest. (H) Subset of (G) where the initial distance to the oral edge is less than four micrometres after the cell division.

Figure 3 PCP orientation by Wnt3 is Wnt/β-catenin-independent, and its propagation across the body axis requires Stbm and Fmi.

(A) Wnt3-rescue with an additional injection of a dominant-negative form of TCF (dnTCF) into the egg, N=10. (B) Wnt3-rescue by the constitutively active form of β-catenin (CA-β-cat) instead of Wnt3 mRNA, N=7. (C) Onset of axial morphology in EG embryos. Localised Wnt3 is necessary and sufficient for the onset of the elongation toward its source. Green: actin (phalloidin), magenta: nuclei (To-Pro3)

and blue: Wnt3-mRNA/Dextran injected cell lineage. (D) Roles of Wnt3 and β-catenin in the axial elongation in LG embryos. The elongation was measured by the elongation index (L/W): the primary axis length (L) divided by its perpendicular length (W), **** $p < 0.0001$, Mann–Whitney U test). Both local Wnt3 expression and β-catenin/TCF-dependent gastrulation were required for axial elongation. See supplementary Figure 3. (E, F) Wnt3-rescue experiments with additional injections of (E) Stbm-MO (N=23) and (F) Fmi-MO (N=6). Radar plots of the PCP orientation show the manually defined proximal area (Proximal: between the dotted line and the Wnt3-positive region) and distal area (Distal: opposite area to the Wnt3-positive region across the dotted line). PCP is correctly polarised without Stbm or Fmi close to the Wnt3-injected cell clone but not in the distant area.

Figure 4. PCP behaviour in Stbm/Fmi-mosaic/ Wnt3-rescue experiments supports the two-step model for global PCP orientation

(A-D) Wnt3-rescued early gastrula embryos, including Stbm(–) or Fmi(–) mosaic patches made by blastomere transplantation. (A, B) blastomeres from Wnt3-MO/Stbm-MO double-injected embryos were transplanted as the doner into Wnt3-rescued host embryos at the 64-cell stage. They happened to be incorporated in close/proximal (A: 658 cells, N=4) or far/distal (B: 757 cells, N=4) positions with respect to the Wnt3 source, respectively. (C, D) The same experiment was conducted with Wnt3-MO/Fmi-MO-injected blastomeres as the donor, incorporated in proximal (C: 984 cells, N=3) and distal (D: 649 cells, N=3) positions, respectively. (E) Schematic drawing of the experimental procedure of the transplantation. (F) Wnt3-rescued early gastrula embryos with Stbm(–) mosaic patch generated by additional injection of Stbm-MO at the 16-cell stage (N=1). (G) Schematic drawing of the experimental procedures for (F). The flow of the PCP orientation is indicated by

grey arrows in the bottom right drawings in (A-D) and right in (G). (H) Graphical summary of Stbm-MO and Fmi-MO mosaic experiments. The graphical representation and thumbnail confocal images indicate Wnt3-positive lineages and Stbm-MO or Fmi-MO-injected lineages in yellow and blue. All vector representations are as in Figure 1.

Figure 5. Mechanical strains can reorient PCP.

(A-E) PCP orientation induced by transplantation from a Wnt3-MO donor into the Wnt3-MO background of a Wnt3-rescue host. A) Incomplete incorporation of host and donor cells into a smooth epidermis (N=3/8) causing long-range PCP orientation, as if the donor acts as an aboral cue, in addition to the Wnt3 oral cue. (A) PCP representation by colour-coded bars. See also the legends for Figure.1 (B) Confocal image of the apical cortex of the epidermis showing the rosette structure caused by incomplete incorporation of the donor cells. Both host and donor cells are elongated around the graft boundary. (C) Graphical summary of the PCP orientation: Wnt3-mRNA lineage in Wnt3-rescue host in yellow, Wnt3-MO graft in blue. (D) 3D reconstruction of the rosette structure from the confocal images by contouring cortical actin signals. (E) Schematic representation of the transplant experiment. (F) 3D representation of the late gastrula morphologies induced by mRNA injection of dominant negative form (RhoABC-DN) and constitutively active forms (RhoABC-CA2) of the PCP effector RhoABC, which caused reduced elongation and extra protrusions, respectively. The overall oral-aboral axis remained distinguishable based on morphology and gastrulation. (G-I) PCP is coordinated consistently with respect to the induced protrusions caused by RhoABC-CA2. (G) Colour-wheel representation of PCP in the RhoABC-CA2 injected early gastrula embryos; the

presumed oral pole is to the top-right. (H) 3D reconstruction of the tissue morphology for the same specimen, with PCP flow represented by arrows. (I) Confocal image of the apical cortex of the epidermis at the induced protrusion, corresponding rectangles in G and H. Cortical actin fibres are circumferentially organised around the protrusion. Bars are 50 µm except for 10 µm in B and I. See Figure 1 for the circular colour-code representation of PCP orientation. cyan: actin; magenta: γ-tubulin; blue: donor lineage marker Dextran for B and I

Figure 6. Models for body axis symmetry-breaking during *Clytia* embryogenesis and PCP-driven axis innovation scenarios in metazoan evolution

(A) Two-step PCP axis orientation by local Wnt3. Local gradients of Wnt3 at the oral end of the *Clytia* embryo orient epidermal cell polarity near the Wnt3-positive area. This process does not require Wnt/β-catenin signalling. Local PCP orientation propagates to the aboral side through the action of core PCP proteins between neighbouring cells. Wnt3 expression is likely maintained by Wnt3/β-catenin feedback regulation. (B) Two possible metazoan body axis evolution scenarios from a choanoblastaea, a multicellular and non-polarised metazoan common ancestor. In the “Wnt/β-catenin-first” scenario (bottom), the choanoblastaea first acquires a mechanism to activate the Wnt/β-catenin pathway locally. Stably locally maintained Wnt ligand expression is then recruited by preexisting but non-directed core Fz/PCP interactions to orient PCP and morphogenesis. In the "PCP-first scenario" (top), the self-organising capacity of core PCP protein interactions creates tissue polarity without any specific cue to specify the direction. The advantage of coordinated

polarity of cilia movement for filter-feeding, swimming or morphology could have favoured directed symmetry breaking using reliable cues. These could have initially been provided by environmental or mechanical constraints before the recruitment of localised Wnt binding to Fz to assure PCP orientation, and then the emergence of downstream beta-catenin signalling.

References

1. Brunet, T., and King, N. (2017). The Origin of Animal Multicellularity and Cell Differentiation. Developmental cell *43*, 124–140. https://doi.org/10.1016/j.devcel.2017.09.016.

2. Nielsen, C. (2008). Six major steps in animal evolution: are we derived sponge larvae? Evolution & development *10*, 241–257. https://doi.org/10.1111/j.1525-142x.2008.00231.x.

3. Sebé-Pedrós, A., Degnan, B.M., and Ruiz-Trillo, I. (2017). The origin of Metazoa: a unicellular perspective. Nat Rev Genet *18*, 498–512. https://doi.org/10.1038/nrg.2017.21.

4. Maldonado, M. (2004). Choanoflagellates, choanocytes, and animal multicellularity. Invertebrate Biology *123*, 1–22. https://doi.org/10.1111/j.1744-7410.2004.tb00138.x.

5. Holstein, T.W., Watanabe, H., and Özbek, S. (2011). Signaling pathways and axis formation in the lower metazoa. Current topics in developmental biology *97*, 137–177. https://doi.org/10.1016/b978-0-12-385975-4.00012-7.

6. Loh, K.M., Amerongen, R. van, and Nusse, R. (2016). Generating Cellular Diversity and Spatial Form: Wnt Signaling and the Evolution of Multicellular Animals. Developmental cell *38*, 643–655. https://doi.org/10.1016/j.devcel.2016.08.011.

7. Petersen, C.P., and Reddien, P.W. (2009). Wnt signaling and the polarity of the primary body axis. Cell *139*, 1056–1068. https://doi.org/10.1016/j.cell.2009.11.035.

8. Jager, M., Dayraud, C., Mialot, A., Quéinnec, E., Guyader, H. le, and Manuel, M. (2013). Evidence for Involvement of Wnt Signalling in Body Polarities, Cell Proliferation, and the Neuro-Sensory System in an Adult Ctenophore. Plos One *8*, e84363. https://doi.org/10.1371/journal.pone.0084363.

9. Reid, P.J.W., Matveev, E., McClymont, A., Posfai, D., Hill, A.L., and Leys, S.P. (2018). Wnt signaling and polarity in freshwater sponges. BMC Evol. Biol. *18*, 12. https://doi.org/10.1186/s12862-018-1118-0.

10. Freeman, G. (1981). The role of Polarity in the Development of the Hydrozoan Planula Larva. Wilhelm Roux's Archives *190*, 168–184.

11. Butler, M.T., and Wallingford, J.B. (2017). Planar cell polarity in development and disease. Nature Reviews Molecular Cell Biology *18*, 375–388. https://doi.org/10.1038/nrm.2017.11.

12. Seifert, J.R.K., and Mlodzik, M. (2007). Frizzled/PCP signalling: a conserved mechanism regulating cell polarity and directed motility. Nat Rev Genet *8*, 126–138. https://doi.org/10.1038/nrg2042.

13. Vladar, E.K., Antic, D., and Axelrod, J.D. (2009). Planar Cell Polarity Signaling: The Developing Cell's Compass. Cold Spring Harbor Perspectives in Biology *1*, a002964–a002964. https://doi.org/10.1101/cshperspect.a002964.

14. Gray, R.S., Roszko, I., and Solnica-Krezel, L. (2011). Planar cell polarity: coordinating morphogenetic cell behaviors with embryonic polarity. Developmental cell *21*, 120–133. https://doi.org/10.1016/j.devcel.2011.06.011.

15. May-Simera, H., and Kelley, M.W. (2012). Planar cell polarity in the inner ear. Current topics in developmental biology *101*, 111–140. https://doi.org/10.1016/b978-0-12-394592-1.00006-5.

16. Hale, R., and Strutt, D. (2015). Conservation of Planar Polarity Pathway Function Across the Animal Kingdom. Annu Rev Genet *49*, 529–551. https://doi.org/10.1146/annurev-genet-112414-055224.

17. Lapébie, P., Borchiellini, C., and Houliston, E. (2011). Dissecting the PCP pathway: one or more pathways?: Does a separate Wnt-Fz-Rho pathway drive morphogenesis? Bioessays *33*, 759–768. https://doi.org/10.1002/bies.201100023.

18. Schenkelaars, Q., Fierro-Constain, L., Renard, E., and Borchiellini, C. (2016). Retracing the path of planar cell polarity. BMC evolutionary biology *16*, 69–13. https://doi.org/10.1186/s12862-016-0641-0.

19. Houliston, E., Leclère, L., Munro, C., Copley, R.R., and Momose, T. (2022). Past, present and future of Clytia hemisphaerica as a laboratory jellyfish. Curr Top Dev Biol *147*, 121–151. https://doi.org/10.1016/bs.ctdb.2021.12.014.

20. Momose, T., and Houliston, E. (2007). Two oppositely localised frizzled RNAs as axis determinants in a cnidarian embryo. PLoS biology *5*, e70. https://doi.org/10.1371/journal.pbio.0050070.

21. Momose, T., Derelle, R., and Houliston, E. (2008). A maternally localised Wnt ligand required for axial patterning in the cnidarian Clytia hemisphaerica. Development (Cambridge, England) *135*, 2105–2113. https://doi.org/10.1242/dev.021543.

22. Momose, T., Kraus, Y., and Houliston, E. (2012). A conserved function for Strabismus in establishing planar cell polarity in the ciliated ectoderm during cnidarian larval development. Development (Cambridge, England) *139*, 4374–4382. https://doi.org/10.1242/dev.084251.

23. Lapébie, P., Ruggiero, A., Barreau, C., Chevalier, S., Chang, P., Dru, P., Houliston, E., and Momose, T. (2014). Differential Responses to Wnt and PCP Disruption Predict Expression and Developmental Function of Conserved and Novel Genes in a Cnidarian. PLoS genetics *10*, e1004590. https://doi.org/10.1371/journal.pgen.1004590.

24. Kraus, Y., Chevalier, S., and Houliston, E. (2020). Cell shape changes during larval body plan development in Clytia hemisphaerica. Developmental biology *468*, 59–79. https://doi.org/10.1016/j.ydbio.2020.09.013.

25. Negishi, T., Miyazaki, N., Murata, K., Yasuo, H., and Ueno, N. (2016). Physical association between a novel plasma-membrane structure and centrosome orients cell division. eLife *5*, e16550. https://doi.org/10.7554/elife.16550.

26. Bellaiche, Y., Beaudoin-Massiani, O., Stuttem, I., and Schweisguth, F. (2004). The planar cell polarity protein Strabismus promotes Pins anterior localization during asymmetric division of sensory organ precursor cells in Drosophila. Development (Cambridge, England) *131*, 469–478.

27. Devenport, D., Oristian, D., Heller, E., and Fuchs, E. (2011). Mitotic internalization of planar cell polarity proteins preserves tissue polarity. Nature cell biology *13*, 893–902. https://doi.org/10.1038/ncb2284.

28. Amonlirdviman, K., Khare, N.A., Tree, D.R.P., Chen, W.-S., Axelrod, J.D., and Tomlin, C.J. (2005). Mathematical modeling of planar cell polarity to understand

domineering nonautonomy. Science *307*, 423–426. https://doi.org/10.1126/science.1105471.

29. Gao, B., Song, H., Bishop, K., Elliot, G., Garrett, L., English, M.A., Andre, P., Robinson, J., Sood, R., Minami, Y., et al. (2011). Wnt signaling gradients establish planar cell polarity by inducing Vangl2 phosphorylation through Ror2. Developmental cell *20*, 163–176. https://doi.org/10.1016/j.devcel.2011.01.001.

30. Minegishi, K., Hashimoto, M., Ajima, R., Takaoka, K., Shinohara, K., Ikawa, Y., Nishimura, H., McMahon, A.P., Willert, K., Okada, Y., et al. (2017). A Wnt5 Activity Asymmetry and Intercellular Signaling via PCP Proteins Polarize Node Cells for Left-Right Symmetry Breaking. Developmental cell *40*, 439-452.e4. https://doi.org/10.1016/j.devcel.2017.02.010.

31. Aigouy, B., Farhadifar, R., Staple, D.B., Sagner, A., Röper, J.-C., Jülicher, F., and Eaton, S. (2010). Cell flow reorients the axis of planar polarity in the wing epithelium of Drosophila. Cell *142*, 773–786. https://doi.org/10.1016/j.cell.2010.07.042.

32. Guirao, B., Meunier, A., Mortaud, S., Aguilar, A., Corsi, J.-M., Strehl, L., Hirota, Y., Desoeuvre, A., Boutin, C., Han, Y.-G., et al. (2010). Coupling between hydrodynamic forces and planar cell polarity orients mammalian motile cilia. Nature cell biology *12*, 341–350. https://doi.org/10.1038/ncb2040.

33. Mitchell, B., Jacobs, R., Li, J., Chien, S., and Kintner, C. (2007). A positive feedback mechanism governs the polarity and motion of motile cilia. Nature *447*, 97–101.

34. Olguin, P., Glavic, A., and Mlodzik, M. (2011). Intertissue mechanical stress affects Frizzled-mediated planar cell polarity in the Drosophila notum epidermis. Current biology : CB *21*, 236–242. https://doi.org/10.1016/j.cub.2011.01.001.

35. Chien, Y.-H., Kim, S., and Kintner, C. (2022). Mechanical strain breaks planar symmetry in embryonic epithelia via polarized microtubules. Cells Dev *170*, 203791. https://doi.org/10.1016/j.cdev.2022.203791.

36. Zallen, J.A. (2007). Planar polarity and tissue morphogenesis. Cell *129*, 1051–1063. https://doi.org/10.1016/j.cell.2007.05.050.

37. Wallingford, J.B. (2012). Planar cell polarity and the developmental control of cell behavior in vertebrate embryos. *28*, 627–653. https://doi.org/10.1146/annurev-cellbio-092910-154208.

38. Kumburegama, S., Wijesena, N., Xu, R., and Wikramanayake, A.H. (2011). Strabismus-mediated primary archenteron invagination is uncoupled from Wnt/β-catenin-dependent endoderm cell fate specification in Nematostella vectensis (Anthozoa, Cnidaria): Implications for the evolution of gastrulation. EvoDevo *2*, 2. https://doi.org/10.1186/2041-9139-2-2.

39. Tada, M., and Smith, J.C. (2000). Xwnt11 is a target of Xenopus Brachyury: regulation of gastrulation movements via Dishevelled, but not through the canonical Wnt pathway. Development (Cambridge, England) *127*, 2227–2238.

40. Heisenberg, C.P., Tada, M., Rauch, G.J., Saúde, L., Concha, M.L., Geisler, R., Stemple, D.L., Smith, J.C., and Wilson, S.W. (2000). Silberblick/Wnt11 mediates convergent extension movements during zebrafish gastrulation. Nature *405*, 76–81. https://doi.org/10.1038/35011068.

41. Wallingford, J.B., and Harland, R.M. (2001). Xenopus Dishevelled signaling regulates both neural and mesodermal convergent extension: parallel forces elongating the body axis. Development (Cambridge, England) *128*, 2581–2592.

42. Kilian, B., Mansukoski, H., Barbosa, F.C., Ulrich, F., Tada, M., and Heisenberg, C.-P. (2003). The role of Ppt/Wnt5 in regulating cell shape and movement during

zebrafish gastrulation. Mechanisms of development *120*, 467–476. https://doi.org/10.1016/s0925-4773(03)00004-2.

43. Gros, J., Serralbo, O., and Marcelle, C. (2009). WNT11 acts as a directional cue to organize the elongation of early muscle fibres. Nature *457*, 589–593. https://doi.org/10.1038/nature07564.

44. Tao, Q., Yokota, C., Puck, H., Kofron, M., Birsoy, B., Yan, D., Asashima, M., Wylie, C.C., Lin, X., and Heasman, J. (2005). Maternal Wnt11 Activates the Canonical Wnt Signaling Pathway Required for Axis Formation in Xenopus Embryos. Cell *120*, 857–871. https://doi.org/10.1016/j.cell.2005.01.013.

45. Witzel, S., Zimyanin, V., Carreira-Barbosa, F., Tada, M., and Heisenberg, C.P. (2006). Wnt11 controls cell contact persistence by local accumulation of Frizzled 7 at the plasma membrane. The Journal of cell biology *175*, 791–802. https://doi.org/10.1083/jcb.200606017.

46. Livshits, A., Shani-Zerbib, L., Maroudas-Sacks, Y., Braun, E., and Keren, K. (2017). Structural Inheritance of the Actin Cytoskeletal Organization Determines the Body Axis in Regenerating Hydra. Cell Rep. *18*, 1410–1421. https://doi.org/10.1016/j.celrep.2017.01.036.

47. Sinigaglia, C., Peron, S., Eichelbrenner, J., Chevalier, S., Steger, J., Barreau, C., Houliston, E., and Leclère, L. (2020). Pattern regulation in a regenerating jellyfish. Elife *9*, e54868. https://doi.org/10.7554/elife.54868.

48. Wu, J., Roman, A.-C., Carvajal-Gonzalez, J.M., and Mlodzik, M. (2013). Wg and Wnt4 provide long-range directional input to planar cell polarity orientation in Drosophila. Nature cell biology *15*, 1045–1055. https://doi.org/10.1038/ncb2806.

49. Yu, J.J.S., Maugarny-Calès, A., Pelletier, S., Alexandre, C., Bellaïche, Y., Vincent, J.-P., and McGough, I.J. (2020). Frizzled-dependent Planar Cell Polarity

without Wnt Ligands. bioRxiv *125*, 2020.05.23.108977. https://doi.org/10.1101/2020.05.23.108977.

50. Chu, C.-W., and Sokol, S.Y. (2016). Wnt proteins can direct planar cell polarity in vertebrate ectoderm. eLife *5*, 940. https://doi.org/10.7554/elife.16463.

51. Kusserow, A., Pang, K., Sturm, C., Hrouda, M., Lentfer, J., Schmidt, H.A., Technau, U., Haeseler, A. von, Hobmayer, B., Martindale, M.Q., et al. (2005). Unexpected complexity of the Wnt gene family in a sea anemone. Nature *433*, 156–160. https://doi.org/10.1038/nature03158.

52. Yang, C., Axelrod, J., and Simon, M. (2002). Regulation of Frizzled by fat-like cadherins during planar polarity signaling in the Drosophila compound eye. Cell *108*, 675–688.

53. Strutt, H., and Strutt, D. (2021). How do the Fat–Dachsous and core planar polarity pathways act together and independently to coordinate polarized cell behaviours? Open Biol *11*, 200356. https://doi.org/10.1098/rsob.200356.

54. Brooun, M., Klimovich, A., Bashkurov, M., Pearson, B.J., Steele, R.E., and McNeill, H. (2020). Ancestral roles of atypical cadherins in planar cell polarity. Proc National Acad Sci *117*, 19310–19320. https://doi.org/10.1073/pnas.1917570117.

55. Byrum, C.A. (2001). An analysis of hydrozoan gastrulation by unipolar ingression. Developmental biology *240*, 627–640. https://doi.org/10.1006/dbio.2001.0484.

56. Sande, M. van der, Kraus, Y., Houliston, E., and Kaandorp, J. (2020). A cell-based boundary model of gastrulation by unipolar ingression in the hydrozoan cnidarian Clytia hemisphaerica. Developmental biology *460*, 176–186. https://doi.org/10.1016/j.ydbio.2019.12.012.

57. Stokkermans, A., Chakrabarti, A., Subramanian, K., Wang, L., Yin, S., Moghe, P., Steenbergen, P., Mönke, G., Hiiragi, T., Prevedel, R., et al. (2022). Muscular hydraulics drive larva-polyp morphogenesis. Curr Biol *32*, 4707-4718.e8. https://doi.org/10.1016/j.cub.2022.08.065.

58. Arendt, D., Benito-Gutierrez, E., Brunet, T., and Marlow, H. (2015). Gastric pouches and the mucociliary sole: setting the stage for nervous system evolution. Philosophical Transactions Royal Soc B Biological Sci *370*, 20150286. https://doi.org/10.1098/rstb.2015.0286.

59. Haeckel, E. (1873). Die Gastraea-Theorie, die phylogenetische Classification des Thierreichs und die Homologie der Keimblätter.

60. Hyman, L.H. (1951). The invertebrates : Platyhelminthes and Rhynchocoela, the acoelomate Bilateria.. (New York : McGraw-Hill Book Company Inc.).

61. Nichols, S.A., Dirks, W., Pearse, J.S., and King, N. (2006). Early evolution of animal cell signaling and adhesion genes. Proc National Acad Sci *103*, 12451–12456. https://doi.org/10.1073/pnas.0604065103.

62. Hoops, H. (1993). Flagellar, cellular and organismal polarity in Volvox carteri. Journal of cell science.

63. Cavalier-Smith, T. (2017). Origin of animal multicellularity: precursors, causes, consequences-the choanoflagellate/sponge transition, neurogenesis and the Cambrian explosion. Philosophical transactions of the Royal Society of London. Series B, Biological sciences *372*, 20150476. https://doi.org/10.1098/rstb.2015.0476.

64. Lechable, M., Jan, A., Duchene, A., Uveira, J., Weissbourd, B., Gissat, L., Collet, S., Gilletta, L., Chevalier, S., Leclère, L., et al. (2020). An improved whole life cycle culture protocol for the hydrozoan genetic model Clytia hemisphaerica. Biology open *9*, bio051268. https://doi.org/10.1242/bio.051268.

65. Korinek, V., Barker, N., Morin, P.J., Wichen, D. van, Weger, R. de, Kinzler, K.W., Vogelstein, B., and Clevers, H. (1997). Constitutive transcriptional activation by a beta-catenin-Tcf complex in APC-/- colon carcinoma. Science *275*, 1784–1787. https://doi.org/10.1126/science.275.5307.1784.

66. Baba, Y., Yokota, T., Spits, H., Garrett, K.P., Hayashi, S.-I., and Kincade, P.W. (2006). Constitutively active beta-catenin promotes expansion of multipotent hematopoietic progenitors in culture. Journal of immunology (Baltimore, Md. : 1950) *177*, 2294–2303. https://doi.org/10.4049/jimmunol.177.4.2294.

67. Weissbourd, B., Momose, T., Nair, A., Kennedy, A., Hunt, B., and Anderson, D.J. (2021). Functional modules within a distributed neural network control feeding in a model medusa. Biorxiv, 2021.02.22.432372. https://doi.org/10.1101/2021.02.22.432372.

68. Berens, P., and 2009 CircStat: A MATLAB Toolbox for Circular Statistics. Journal of Statistical Software *31*.

Figure 1

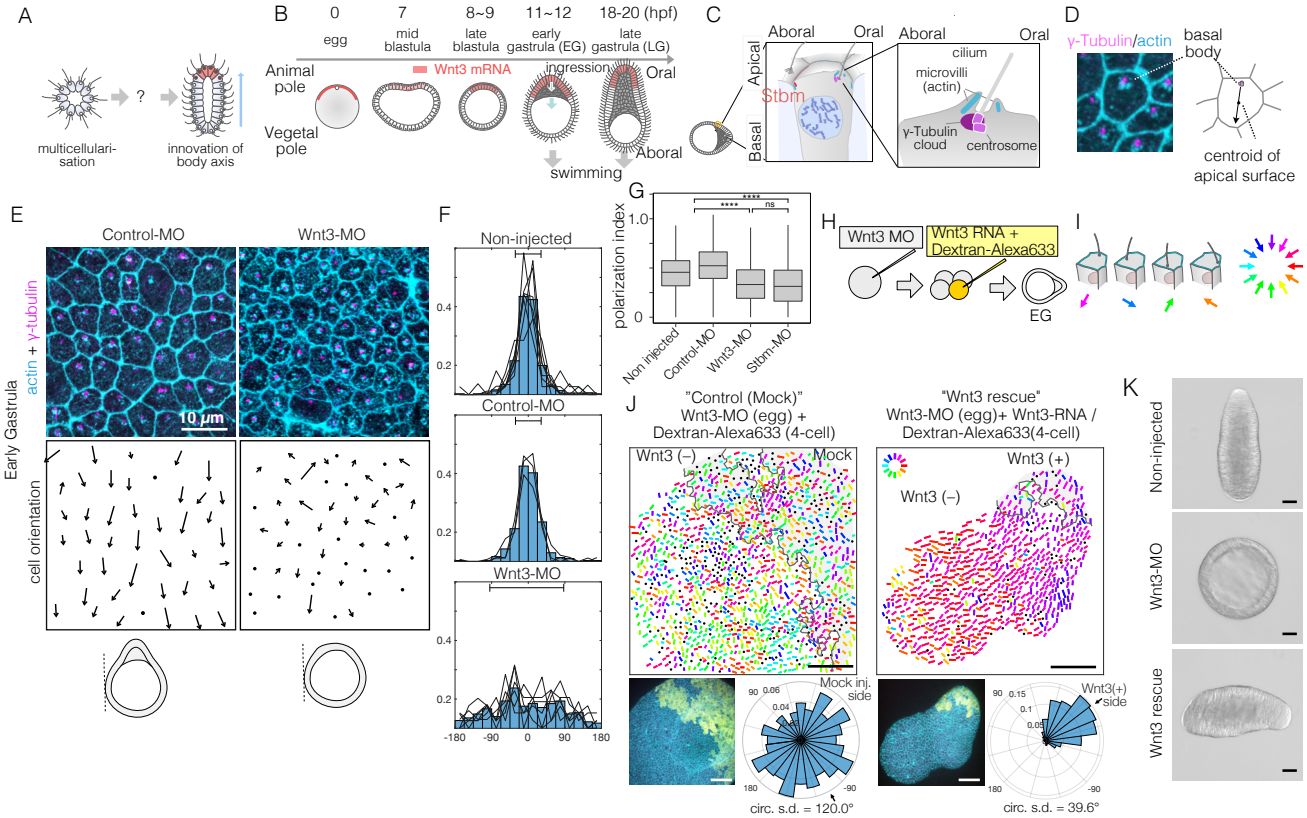
A
multicellularisation
innovation of body axis
B
0
egg
7
mid blastula
8~9
late blastula
11~12
early gastrula (EG)
18-20 (hpf)
late gastrula (LG)
Animal pole
Vegetal pole
Wnt3 mRNA
ingression
Oral
Aboral
swimming
C
Aboral
Oral
Apical
Basal
Stbm
cilium
microvilli (actin)
γ-Tubulin cloud
centrosome
D
γ-Tubulin/actin
basal body
centroid of apical surface
E
Control-MO
Wnt3-MO
actin + γ-tubulin
Early Gastrula
cell orientation
10 μm
F
Non-injected
Control-MO
Wnt3-MO
G
polarization index
Non injected
Control-MO
Wnt3-MO
Stbm-MO
H
Wnt3 MO
Wnt3 RNA + Dextran-Alexa633
EG
I
J
"Control (Mock)"
Wnt3-MO (egg) + Dextran-Alexa633 (4-cell)
"Wnt3 rescue"
Wnt3-MO (egg)+ Wnt3-RNA / Dextran-Alexa633(4-cell)
Wnt3 (–)
Mock
Wnt3 (+)
Mock inj. side
Wnt3(+) side
circ. s.d. = 120.0°
circ. s.d. = 39.6°
K
Non-injected
Wnt3-MO
Wnt3 rescue

Figure 2

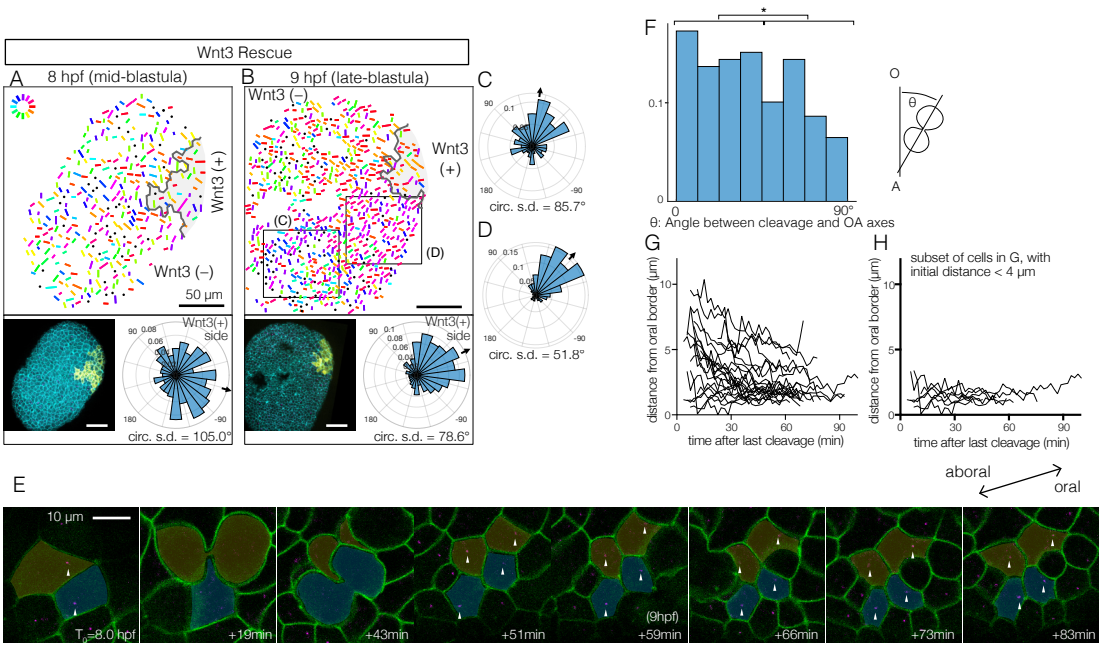
Wnt3 Rescue
A
8 hpf (mid-blastula)
Wnt3 (+)
Wnt3 (–)
50 µm
Wnt3(+) side
circ. s.d. = 105.0°
B
9 hpf (late-blastula)
Wnt3 (–)
Wnt3 (+)
(C)
(D)
Wnt3(+) side
circ. s.d. = 78.6°
C
circ. s.d. = 85.7°
D
circ. s.d. = 51.8°
F
θ: Angle between cleavage and OA axes
O
A
G
distance from oral border (µm)
time after last cleavage (min)
H
subset of cells in G, with initial distance < 4 µm
distance from oral border (µm)
time after last cleavage (min)
aboral
oral

E

10 µm
T0 -8.0 hpf
+19min
+43min
+51min
(9hpf)
+59min
+66min
+73min
+83min

Figure 3

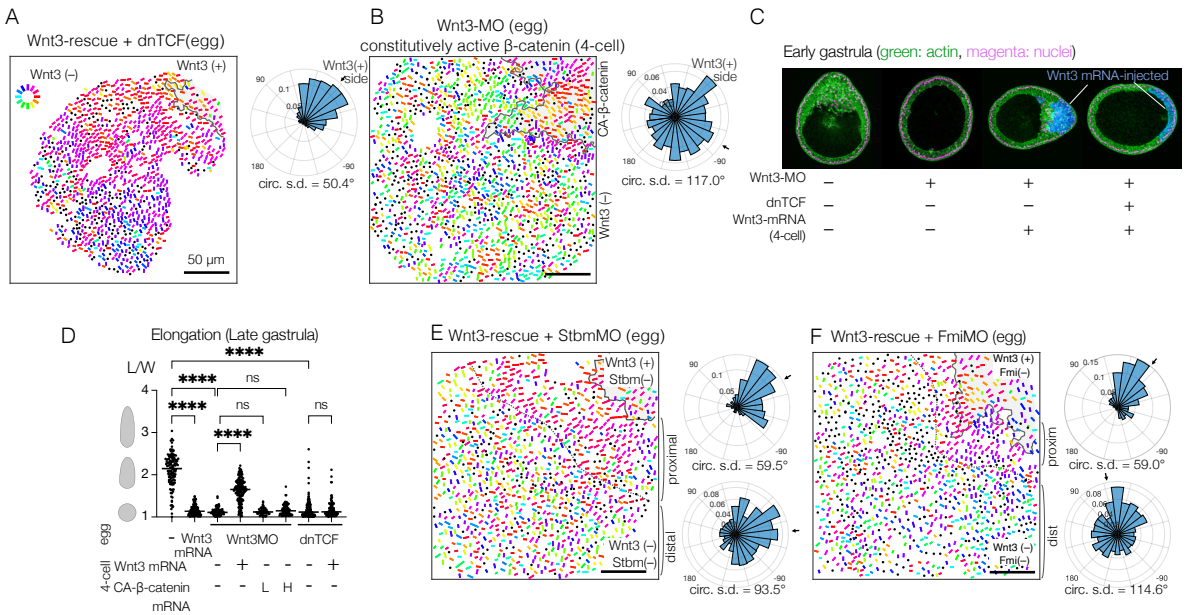
A
Wnt3-rescue + dnTCF(egg)
Wnt3 (–)
Wnt3 (+)
50 µm
Wnt3(+) side
circ. s.d. = 50.4°
B
Wnt3-MO (egg)
constitutively active β-catenin (4-cell)
CA-β-catenin
Wnt3 (–)
Wnt3(+) side
circ. s.d. = 117.0°
C
Early gastrula (green: actin, magenta: nuclei)
Wnt3 mRNA-injected
Wnt3-MO – + + +
dnTCF – – – +
Wnt3-mRNA (4-cell) – – + +
D
Elongation (Late gastrula)
L/W
egg
4-cell
Wnt3 mRNA
Wnt3MO
dnTCF
Wnt3 mRNA - + - - - +
CA-β-catenin mRNA - - L H - -
E Wnt3-rescue + StbmMO (egg)
Wnt3 (+) Stbm(–)
Wnt3 (–) Stbm(–)
proximal
distal
circ. s.d. = 59.5°
circ. s.d. = 93.5°
F Wnt3-rescue + FmiMO (egg)
Wnt3 (+) Fmi(–)
Wnt3 (–) Fmi(–)
proxim
dist
circ. s.d. = 59.0°
circ. s.d. = 114.6°

Figure 4

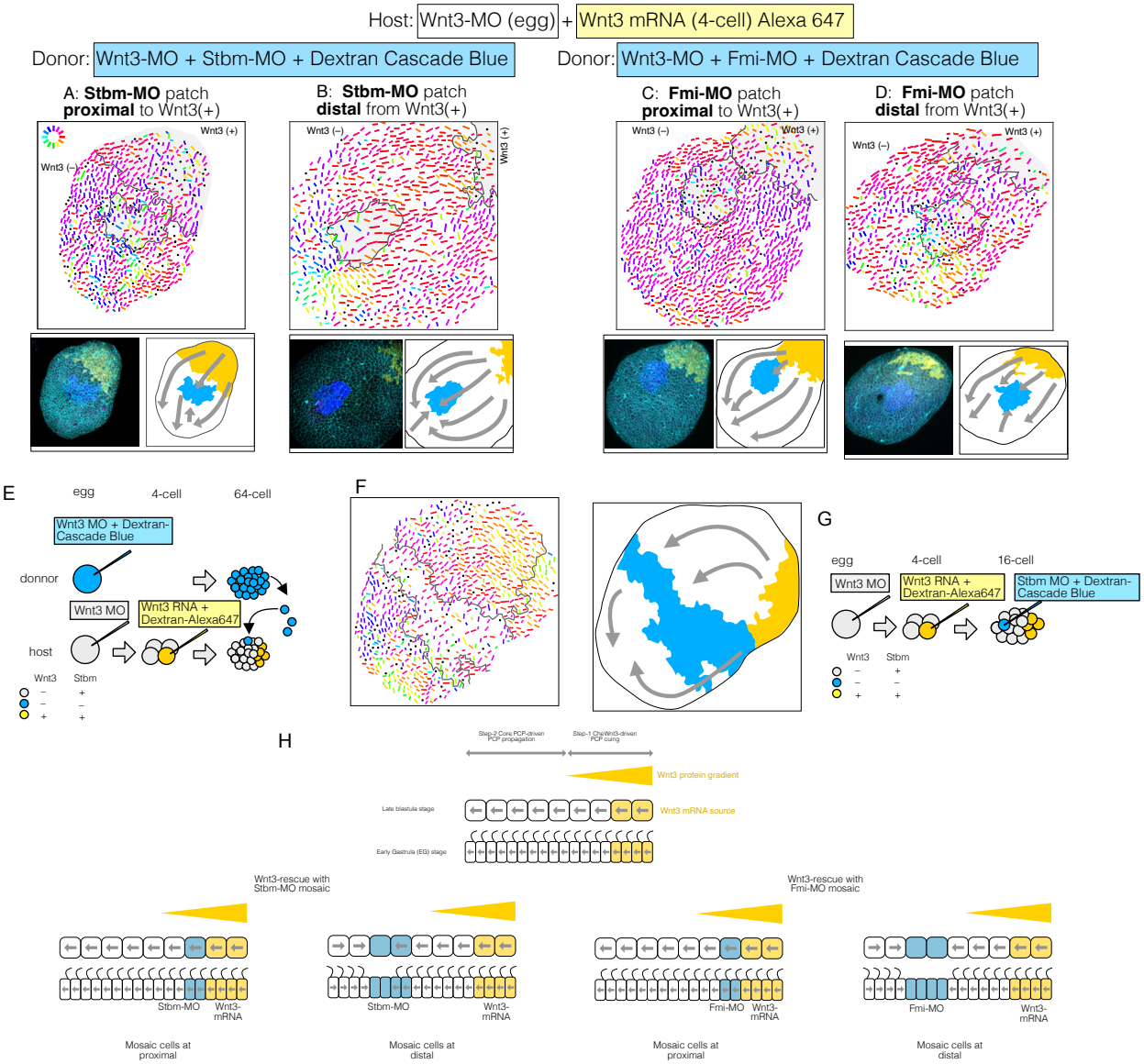
Host: Wnt3-MO (egg) + Wnt3 mRNA (4-cell) Alexa 647
Donor: Wnt3-MO + Stbm-MO + Dextran Cascade Blue
Donor: Wnt3-MO + Fmi-MO + Dextran Cascade Blue
A: Stbm-MO patch proximal to Wnt3(+)
B: Stbm-MO patch distal from Wnt3(+)
C: Fmi-MO patch proximal to Wnt3(+)
D: Fmi-MO patch distal from Wnt3(+)
Wnt3 (+)
Wnt3 (–)
E
egg
4-cell
64-cell
Wnt3 MO + Dextran-Cascade Blue
donnor
Wnt3 MO
Wnt3 RNA + Dextran-Alexa647
host
Wnt3
Stbm
F
G
egg
4-cell
16-cell
Wnt3 MO
Wnt3 RNA + Dextran-Alexa647
Stbm MO + Dextran-Cascade Blue
Wnt3
Stbm

H
Step-2 Core PCP-driven PCP propagation
Step-1 Che/Wnt3-driven PCP caring
Wnt3 protein gradient
Late blastula stage
Wnt3 mRNA source
Early Gastrula (EG) stage
Wnt3-rescue with Stbm-MO mosaic
Wnt3-rescue with Fmi-MO mosaic
Stbm-MO
Wnt3-mRNA
Fmi-MO
Mosaic cells at proximal
Mosaic cells at distal

Figure 5

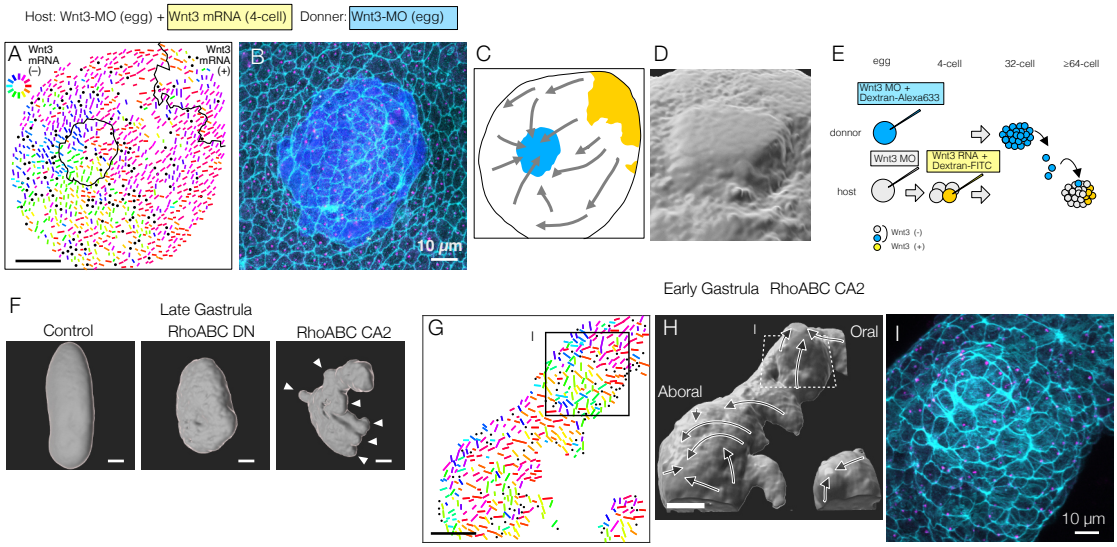
Host: Wnt3-MO (egg) + Wnt3 mRNA (4-cell)
Donner: Wnt3-MO (egg)
A
Wnt3 mRNA (–)
Wnt3 mRNA (+)
B
10 µm
C
D
E
egg
4-cell
32-cell
≥64-cell
Wnt3 MO + Dextran-Alexa633
donnor
Wnt3 MO
Wnt3 RNA + Dextran-FITC
host
Wnt3 (-)
Wnt3 (+)
F
Control
Late Gastrula
RhoABC DN
RhoABC CA2
G
Early Gastrula RhoABC CA2
H
Oral
Aboral
I
10 µm

Figure 6

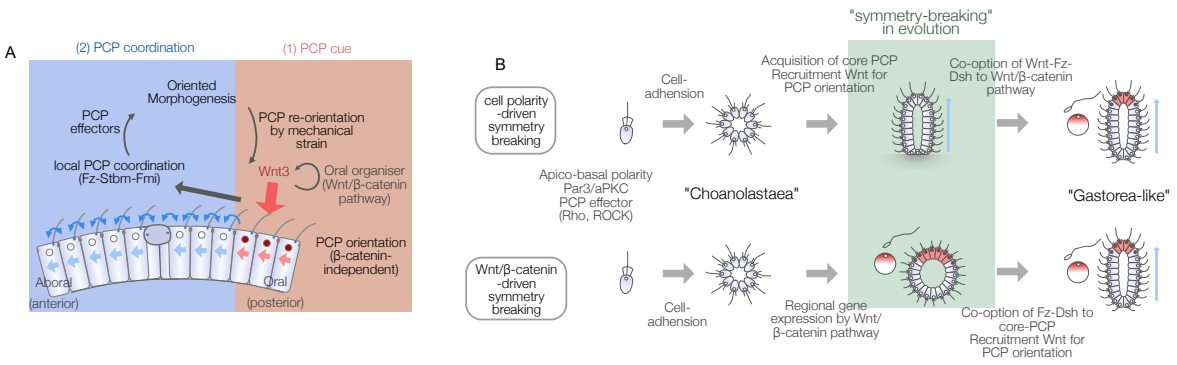
A
(2) PCP coordination
(1) PCP cue
Oriented Morphogenesis
PCP effectors
PCP re-orientation by mechanical strain
local PCP coordination (Fz-Stbm-Fmi)
Wnt3
Oral organiser (Wnt/β-catenin pathway)
PCP orientation (β-catenin-independent)
Aboral
(anterior)
Oral
(posterior)
B
"symmetry-breaking" in evolution
cell polarity -driven symmetry breaking
Cell-adhension
Acquisition of core PCP Recruitment Wnt for PCP orientation
Co-option of Wnt-Fz-Dsh to Wnt/β-catenin pathway
Apico-basal polarity Par3/aPKC PCP effector (Rho, ROCK)
"Choanolastaea"
"Gastorea-like"
Wnt/β-catenin -driven symmetry breaking
Cell-adhension
Regional gene expression by Wnt/β-catenin pathway
Co-option of Fz-Dsh to core-PCP Recruitment Wnt for PCP orientation